redin Revista Facultad de Ingeniería, Universidad de Antioquia, No. 76, pp. 123-133, 2015

# Relevance of the hyperelastic behavior of cruciate ligaments in the modeling of the human knee joint in sagittal plane

UNIVERSIDAD DE ANTIOQUIA 1803

## Relevancia del comportamiento hiperelástico de los ligamentos cruzados en el modelaje de la rodilla humana en el plano sagital

**Daniel Alejandro Ponce-Saldias[1*], Daniel Martins[1], Carlos Rodrigo de Mello-Roesler[2], Otavio Teixeira-Pinto[2], Eduardo Alberto Fancello[2]**

[1]Departamento de Engenharia Mecânica, Universidade Federal de Santa Catarina. Campus Reitor João David Ferreira Lima. CEP: 88040-900. Florianópolis, Brasil.
[2]Laboratório de Engenharia Biomecânica (LEBm), Universidade Federal de Santa Catarina. Campus Reitor João David Ferreira Lima. CEP: 88040-900. Florianópolis, Brasil.

**ARTICLE INFO**
Received July 16, 2014
Accepted May 21, 2015

**KEYWORDS**
Knee modeling, preoperative planning, mechanisms, Davies' method, hyperelastic behavior

Modelaje de la rodilla, planeamiento preoperatorio, mecanismos, método de Davies, comportamiento hiperelástico

**ABSTRACT:** The rupture of the anterior cruciate ligament (ACL) is the most common injury of the human knee. When surgery is required, it is helpful for orthopedic surgeons to scientifically define the best position for the graft, which approximates the functionality of an intact ACL. To accomplish that, it is crucial to estimate the force acting on the ligament (or graft) in response to an external load applied to the knee. This force is called the in-situ force. The objective of this research is to evidence the relevance of the hyperelastic behavior of cruciate ligaments in the two-dimensional modeling of the knee. To achieve this, a sequential method of modeling is proposed based on the theory of mechanisms and Davies' method. In a first approach the cruciate ligaments are treated as rigid bodies, and in a second approach, as hyperelastic bodies. These two approaches are then compared. The model provides information to assist the preoperative planning, by simulation of the ACL positions and in-situ forces. The proposed methodology consists of four steps and an experimental procedure performed by a robotic manipulator to obtain the in-situ forces. Experimental in-situ forces are used to validate the proposed model. Besides helping the preoperative planning, the model allows verifying two relevant biomechanical hypotheses: 1. During the simulation of the ACL in-situ force, the modeling of the cruciate ligaments as rigid links shows similar results to the modeling, which considers the hyperelastic behavior (more complex). 2. The ACL in-situ force can be well approximated when the knee is modeled as a two-dimensional four bar mechanism. Based on the results it can be concluded that the forces obtained by simulations that consider the hyperelastic behavior of the cruciate ligaments are close to the forces obtained by simulations that consider the cruciate ligaments as rigid bodies. It can also be noted that the simulated results are quite similar to the experimental results, which is important considering that the proposed model is simplified.

**RESUMEN:** La ruptura del ligamento cruzado anterior (LCA) es la lesión más común de la rodilla humana. Cuando se requiere cirugía, es de mucha ayuda para los cirujanos definir científicamente el mejor punto de inserción del injerto, para que pueda tener una funcionalidad similar a la de un LCA intacto. Para esto, es crucial la estimación de la fuerza que actúa en el ligamento (o injerto) en respuesta a una carga externa aplicada sobre la rodilla. Esta fuerza es llamada fuerza in-situ. El objetivo de esta investigación es evidenciar la relevancia del comportamiento hiperelástico de los ligamentos cruzados en el modelaje bidimensional de la rodilla. Para ello, se propone una metodología secuencial de modelaje basándose en teoría de mecanismos y el método de Davies. En una primera aproximación, los ligamentos cruzados son considerados como cuerpos rígidos; en una segunda aproximación, como cuerpos con comportamiento hiperelástico. Esas dos aproximaciones son comparadas. El modelo proporciona informaciones que permiten asistir el planeamiento

* Corresponding author: Daniel Alejandro Ponce Saldias
E-mail: danielpo25@gmail.com
ISSN 0120-6230
e-ISSN 2422-2844



DOI: 10.17533/udea.redin.n76a15

pre-operatorio, mediante la simulación de las posiciones y la fuerzas in-situ del LCA. La metodología propuesta consiste en cuatro pasos y considera un procedimiento experimental realizado mediante un manipulador robótico que obtiene las fuerzas in-situ. Las fuerzas in-situ experimentales son usadas para validar el modelo propuesto. Además de apoyar al planeamiento pre-operatorio, el modelo permite verificar dos hipótesis biomecánicas relevantes: 1. Para la simulación de la fuerza in-situ del LCA, el modelaje de los ligamentos cruzados como barras rígidas, presenta resultados semejantes a los del modelaje que considera el comportamiento hiperelástico (más elaborado). 2. Las fuerzas in-situ del LCA pueden ser aproximadas satisfactoriamente, cuando la rodilla es modelada como un mecanismo bidimensional de 4-barras. Con base en los resultados puede concluirse que las fuerzas obtenidas por simulaciones que consideran el comportamiento hiperelástico de los ligamentos cruzados, son muy próximas a aquellas fuerzas obtenidas en simulaciones que consideran los ligamentos cruzados como cuerpos rígidos. También se puede observar que los resultados simulados son bastante similares a los resultados experimentales, lo que es relevante considerando que el modelaje propuesto es simplificado.

# 1. Introduction

The rupture of the anterior cruciate ligament (ACL) is the most common injury of the human knee [1] causing considerable knee instability, decreasing functional ability and degeneration of adjacent anatomical structures. Surgical treatments for such injuries involve knee joint surgery, where orthopedic surgeons must plan the surgical procedure in order to optimize postoperative results. Therefore, the preoperative planning is a critical step in selecting the surgical technique and the parameter definitions to be used in the surgery for each patient and, thus, it can directly affect the outcome of the surgery.

For an appropriate preoperative planning, the orthopedic surgeon needs to know the exact problem to be solved [2, 3], possible surgical solutions [2, 3] and the expected consequences for each solution [2]. In this context, several studies have been carried out to define mechanical models representative of the knee [2-5]. It has been shown that these models provide orthopedic doctors with additional information regarding several aspects of the preoperative planning, as well as the reconstruction of ligaments, joint surfaces and osteotomy [2]. Moreover, these mechanical models are essential for the design of prostheses [3-5], synthesis of orthoses [3], and the indirect estimation of unmeasured internal forces of the joint [5].

However, orthopedic surgeons also need to perform other tasks, such as: to determine scientifically the point for the insertion of the graft that approximates the functionality of an intact ACL; to ascertain the pretension that the graft should be fixed at; and to estimate the force acting on the ligament (or graft) in response to a load applied to the knee. This force is called the in-situ force [6, 7].

The main aim of this study was to support the orthopedic surgeon in the above-mentioned tasks, using the information provided by a two-dimensional model of the knee. The model was developed based on the mechanism theory, the screw theory and the Davies' method [8-10]. This model allows us to simulate the positions and forces of a healthy ACL in the sagittal plane, considering the hyperelastic behavior of the cruciate ligaments. For this reason the proposed modeling is an improvement of other models described in the literature, which just consider the ligaments as rigid links [11] or elastic links [12]. Moreover, for the in-situ force simulation, the proposed methodology shows evidences that confirm the hypotheses of the cruciate ligaments being considered as rigid and inextensible links, neglecting its hyperelastic behavior. Also, the proposed methodology allows the forces that occur in an ACL graft to be simulated according to the site of the graft insertion.

This paper begins with the proposed methodology for the modeling, which consists of four sequential steps: (1) schematic representation of the physical model of the knee (where the geometric model is established); (2) obtainment of the successive positions of the cruciate ligaments (where the positions are modeled during the flexion movement); (3) determination of the cruciate ligament forces (where the force is acting on the cruciate ligaments for each position); and (4) consideration of hyperelastic behavior (where the force is related with the ligament's strain by means of experimental curves). In order to validate the proposed model, the simulated values for the in-situ force in the ACL are compared with the experimental data previously obtained in [7]. Finally, the conclusions are presented.

# 2. Proposed methodology

The proposed methodology for modeling the knee in the sagittal plane provides a unique and systematic approach consisting in four steps: (1) schematic representation of the physical model of the knee, (2) obtainment of the successive positions of the cruciate ligaments, (3) determination of the cruciate ligament forces, and (4) consideration of hyperelastic behavior.

The first step identifies the initial positions of the cruciate ligaments when the knee is in the full extension position, based on magnetic resonance imaging (MRI). In this step, modeling assumptions are established. The second step leads to the obtainment of the successive positions of the cruciate ligaments in the flexion-extension movement of the knee, using matrix tools. The third step leads to the identification of the forces acting on the cruciate ligaments for each position, by means of the Davies' method. This static analysis enables the in-situ force of the ACL (or ACL

graft) to be obtained, caused by an applied external load. The fourth step leads to the identification of forces considering hyperelastic behavior for the cruciate ligaments. This is performed with the in-situ force, obtained in the previous step, and a constitutive relationship obtained from experimental stress-strain curves [13]. Finally, the effect of the hyperelastic behavior can be analyzed. This whole procedure is briefly schematized in Figure 1 and will be explained in detail below.

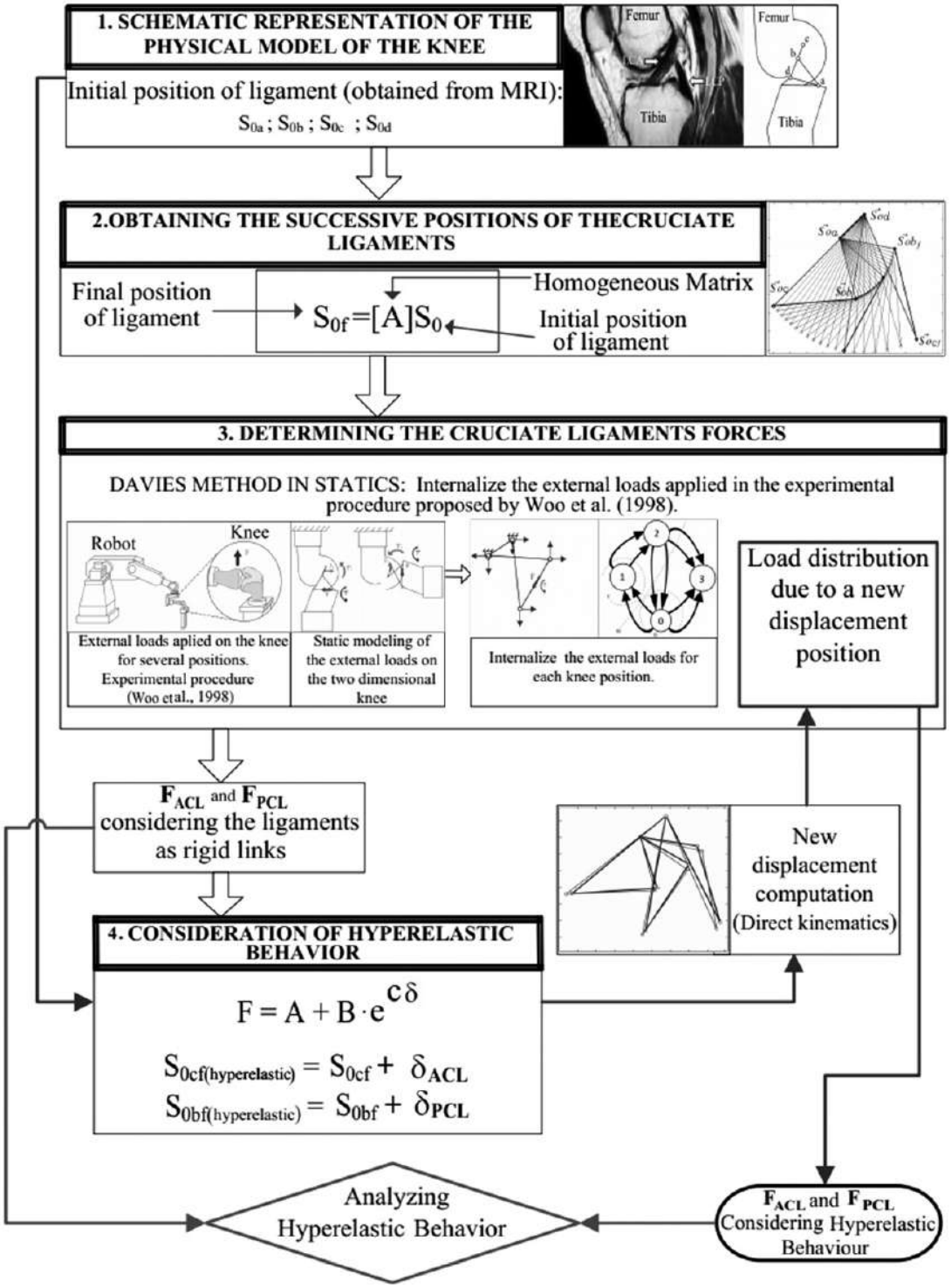


**Figure 1** Schematic process of the proposed methodology, composed of four steps: (1) schematic representation of the physical model of the knee, (2) obtainment of the successive positions of the cruciate ligaments, (3) determination of the cruciate ligament forces, and (4) consideration of hyperelastic behavior

## 2.1. Schematic representation of the physical model of the knee in the sagittal plane

The proposed physical model is based on the experimental approach presented in [14], where is considered that the cruciate ligaments are always under tension and do not change the length while the femoral condyles stay in contact with the tibial condyles. From here, a two-dimensional cross four-bar mechanism abcd is superimposed on to the cruciate ligaments, since the tibia and femur are also considered as rigid links, as shown in Figure 2 (a).

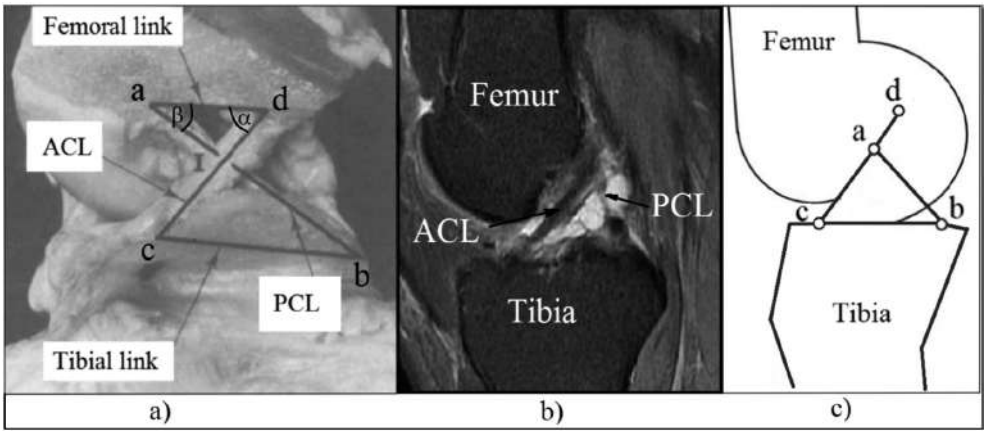


**Figure 2 a) Knee in flexion with a cross four-bar mechanism superimposed on the cruciate ligaments, based on [14]. b) MRI of a knee in extension. c) Physical model of the knee in extension based in [15] where the femoral link ad is collinear to the ACL link cd**

In Figure 2 (a) the point *a, b, c* and *d* are rotary joints of the mechanism, the link *ab* represents the PCL, *cd* represents the ACL, ad represents the femoral link (fixed to the femur) and *bc* represents the tibial link (fixed to the tibia). The angle $\alpha$ indicates the orientation of the link cd relative to the femoral link, and $\beta$ is the orientation angle of the link ab relative to the femoral link. I is the intersection of the cruciate ligaments and represents the center of rotation of the joint. The changing position of the cross four-bar mechanism over the flexion range represents the observed pattern of rolling and sliding of the femur on the tibia for flexion [14]. Furthermore, it is indicated that the shape of the condyles is geometrically defined by the length of the cruciate ligaments, their length ratio and their insertion localization [14].

In agreement with the premises presented in [14], the following assumptions are here considered:

- The human knee is modeled as a two-dimensional four bar mechanism with rigid links.
- All bundles of each cruciate ligament are shrinked in a unique link, during the whole motion.
- The insertion regions of each ligament are considered as a single insertion point during the whole motion, and are used to define the four bar mechanism (points *a, b, c, d*).
- The articular surfaces are considered as undeformable.
- There is no mechanical contribution from collateral ligaments neither from menisci or other structures

The length and position of the links in the proposed model are dependent on the length of ACL and PCL, as well as the location of the ligament insertions on the tibia and femur. These parameters can be determined by MRI inspection of the knee at full extension as shown in Figure 2 (b), where both ACL and PCL appear. The points *a,b,c,d* are located approximately at the middle of the insertion regions of both ligaments. In Figure 2 (c) the physical representation of the knee in extension based on the MRI is shown.

An extensive literature review [16-20] revealed the wide range of variation in the lengths of the cruciate ligaments in the sagittal plane. Based on this literature review and on MRI inspection, the ligament length values chosen for the simulation of the proposed model are: ACL (*cd*)=37mm, PCL (*ab*)=17mm, femoral link (*bc*)=10mm, tibial link (*ad*)=25mm.

## 2.2. Obtainment of the successive positions of the cruciate ligaments

In this section, the successive positions of the cruciate ligaments are calculated, from the maximum extension up to the maximum flexion of the knee ($0^0$ - $140^0$), as shown in Figure 3.

For this analysis, the Freudenstein equation [21] and rigid transformations [22] are used. The Freudenstein equation [21] is widely used for the synthesis of 4-bar mechanisms and in the proposed model it allows us to obtain the $\beta$ angle as a function of $\alpha$ angle (Figure 2 (a)).

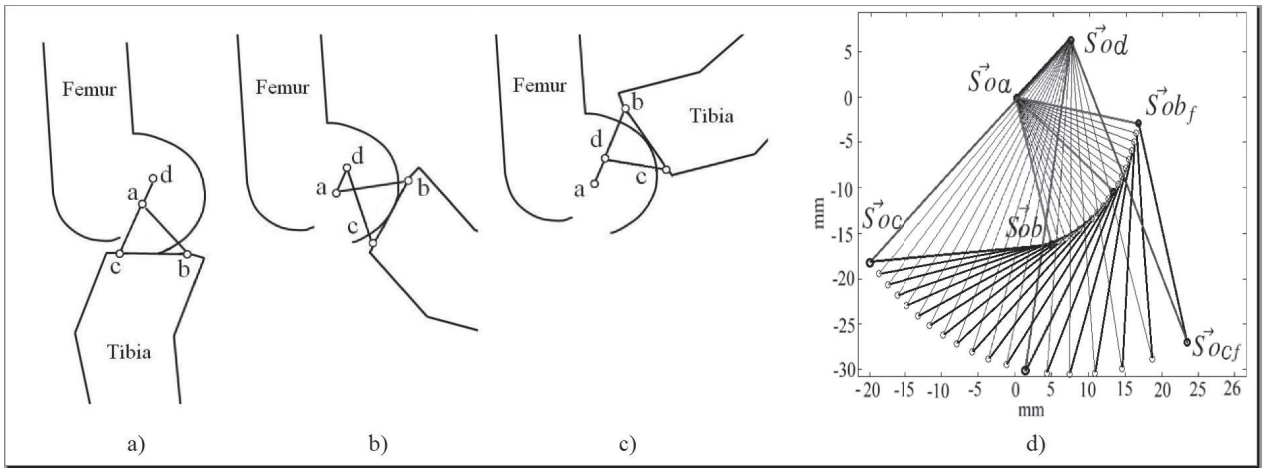


**Figure 3** Mechanical model of the knee in flexion: a) 0° or fully extended, b) 70°, c) 140°, d) Successive positions of the cruciate ligaments for the flexion knee movement, where ACL is in light line between $\vec{So}_c$ and $\vec{So}_d$ screw points, LCP in light line between $\vec{So}_a$ and $\vec{So}_b$ screw points, tibial and femoral link are in dark lines. The femoral link is fixed

Considering the fixed points a and d, and the point a as the origin of the coordinate system, the successive positions of the links ab and cd can be described. The position of the vector ab is described as the rotation of point b around point a, as shown in Eq. (1):

$$\vec{So}_{b_f} = [A_\beta]\vec{So}_b \quad (1)$$

where $\vec{So}_{b_f}$ is the final position of point b, $\vec{So}_b$ is the initial position of point b and $[A_\beta]$ is the homogeneous matrix that describes the rotation angle $\beta$ around point *a*.

In the same way, the position vector cd is described as the rotating point c around point d, as shown in Eq. (2):

$$\vec{So}_{c_f} = [A_\alpha]\vec{So}_c \quad (2)$$

where $\vec{So}_{c_f}$ is the final position of point c, $\vec{Soc}$ is the initial position of point c, and $[A_\alpha]$ is the homogeneous matrix that describes the rotation angle $\alpha$ around point *d*.

On entering the successive values of $\alpha$ (from the maximum extension up to the maximum flexion) in Eqs. (1) and (2), all positions of the cruciate ligaments are obtained, as shown in Figure 3 (d).

## 2.3. Determination of the cruciate ligament forces

In this section the forces in the cruciate ligaments are calculated by static analysis using the Davies' cutset law [8, 9]. The experimental procedure proposed in [7] is modeled and simulated. In this context, the experimental results are used to compare the simulated results. In [7] the in-situ force of the ACL is obtained by using a robotic manipulator system (Unimate, PUMA model 762) and a universal force-moment sensor UFS (JR3, model 4015), as shown in Figure 4 (a).

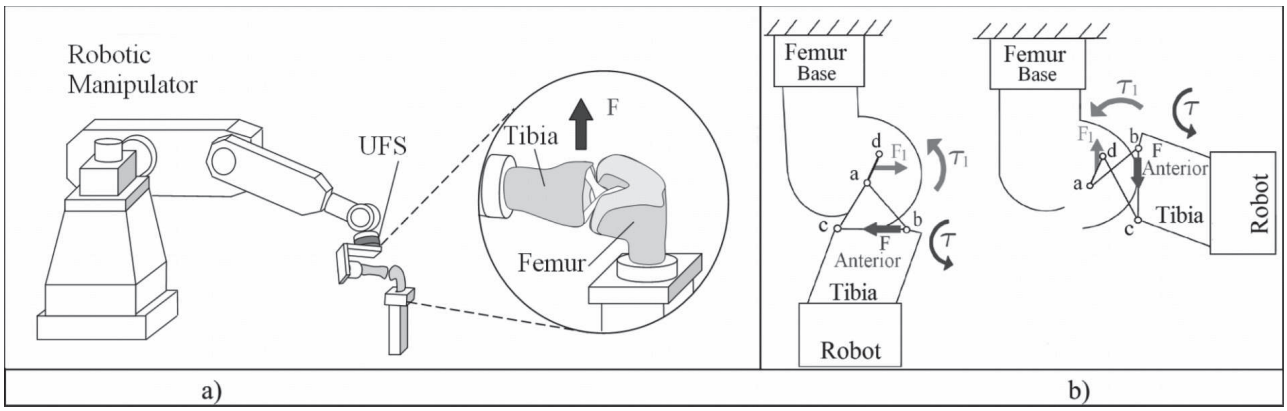


**Figure 4** a) Experimental procedure proposed in [7]. b) Static modeling of the experimental procedure lines. The femoral link is fixed

A brief description of the experimental procedure is performed in order to understand the modeling process and the acting forces. In this experimental procedure, knee specimens where analyzed. The femur was fixed to the ground by a supportive base and the tibia was fixed to the UFS, which in turn is fixed onto the end-effector of the robot (Figure 4 (a)). To obtain the in-situ force of the ACL, the robot applies an anterior tibial load as shown by the dark arrow in Figure 4 (a), and it is applied to five different knee angles of flexion (0°; 15°; 30°; 60°; 90°).

The load direction is chosen anteriorly to the tibia because there are examinations, where the doctor manually applies a similar load to the tibia in order to determine the presence of ACL injuries (Drawer Test, Lachman test). Moreover, the ACL stops the anterior displacement of the tibia relative to the femur. Therefore, the load applied by the robot directly affects the ACL. The UFS sensor records the force and torque data in the tibia and through Jacobian operations the magnitudes of these factors that occur in the ACL are determined, such as the in-situ force [1, 6, 7].

The modeling of the experimental procedure related in [7] is shown in Figure 4 (b). This model adopts the inertial reference system coinciding with point a, belonging to the femur, assuming that the tibia is moving and the femur is fixed.

The anterior tibial force applied by the robot has a magnitude of F, and is accompanied by a torque $\tau$ that constrains theflexion angle in order to provoke a forward translation of the tibia relative to the femur. The loads applied by the robot are shown in dark arrows (Figure 4 (b)). The application point of the force F is called $\vec{S}o_F$, and it is considered to be located at the midpoint of the tibial link bc. The ligaments transmit the loads applied by the robot from the tibia to the femur in the form of a reaction force $F_1$ and a reaction torque $\tau_1$ (Figure 4 (b)).

In [11, 12] the human knee modeling using Davies' method [8-10] was proposed. The static analysis of this work is based on previous works [11, 12]. The external force and torque as shown in dark arrows (Figure 4 (b)), must be internalized and replaced with equivalent actions (reactions forces) [8-10] between links belonging to the mechanism analyzed, resulting in a constrained chain (Figure 5 (a)).

At this stage, numbers are assigned to each link and internal actions $R_x$ and $R_y$ are specified at each joint, as well as the force F and the torque $\tau$ (Figure 5 (a)).

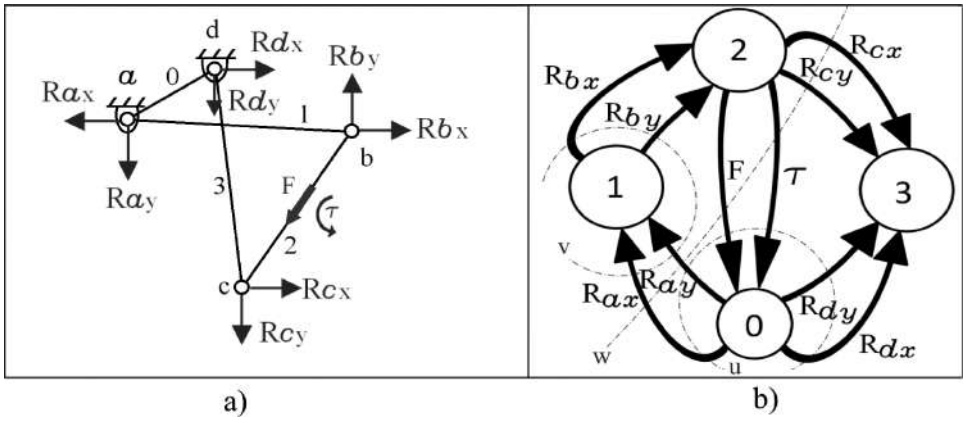


**Figure 5 a) Actions on the couplings of the modeled mechanism. b) Action graph (GA) of the modeled mechanism and k cuts (dashed lines)**

Once the actions are internalized, the action graph called GA (Figure 5 (b)) is constructed [8], where the 8 edges $R_x$ and $R_y$ represent the passive actions between each link in 0, 1, 2 and 3, and the edges F and $\tau$ represent the active actions between links 0 and 2.

To apply the Davies' *cutset law*, k cuts must be determined on the graph GA. The number of k cuts is given in Eq. (3) [23]:

$$k = n - 1 = 4 - 1 = 3 \tag{3}$$

where *n* is the number of vertices of the graph GA. Based on the graph, it is possible to determine the location where *k* = 3 cuts in the graph will be applied [8-10]. The 3 cuts are named *u, v* and *w*, and are shown in dashed lines (Figure 5 (b)).

For the internalized actions chain, in the workspace $\lambda = 3$, $\lambda \cdot k$ equations can be described which must be satisfied by *C* unknowns. The *C* unknowns correspond to the sum of the number of passive and active actions as shown in Eq. (4):

$$C = R_x + R_y + F + \tau = 4 + 4 + 1 + 1 = 10 \tag{4}$$

where the passive actions are $R_x$ and $R_y$ of each joint, and the active actions are *F* and $\tau$. These *C* unknowns can be written as a function of $C_N$ primary variables [10], as shown in Eq. (5).

$$C_N = C - \lambda \cdot k = 10 - (3 \cdot 3) = 1 \tag{5}$$

Thus, it is possible to determine the internal actions *C* of the chain by imposing $C_N$ = 1 variables, corresponding to the force *F*.

A screw that represents forces and torques of a constrained chain is called wrench [8, 9]. In relation to the wrench that represent pure force, e.g. $R_x$ and $R_y$ (in the rotary joints) and the force *F*, the pitch *h* is zero [10], therefore wrenches that represent pure force constraints are shown in Eq. (6) [11, 12].

$$\$ = \left(\vec{So} \times \vec{S}; \vec{S}\right)^T = \left(\vec{So} \times \vec{R}; \vec{R}\right)^T \quad (6)$$

where \$ is the wrench, $\vec{So}$ and $\vec{S}$ are the position and the orientation of the wrench axis, respectively, and $\vec{R}$ is the force.

On the other hand, the wrench pitch corresponding to pure torque $\tau$ is infinite [10]; therefore, wrenches, which represent pure torque are obtained as indicated in Eq. (7) [11, 12].

$$\$ = \left(\vec{So}; 0\right)^T = \left(\tau; 0\right)^T \quad (7)$$

Considering Eqs. (6) and (7), and that the position vectors $\vec{So}$ of the wrenches are obtained in step 2 of the methodology (obtainment of the successive positions of the cruciate ligaments), the wrenches shown in Eq. (8) are obtained by the proposed model:

$$\$_{b_y} = \begin{pmatrix} \vec{So}_{b_f} \times \vec{R}_{b_y} \\ \vec{R}_{b_y} \end{pmatrix}; \$_{c_x} = \begin{pmatrix} \vec{So}_{c_f} \times \vec{R}_{c_x} \\ \vec{R}_{c_x} \end{pmatrix}; \$_{c_y} = \begin{pmatrix} \vec{So}_{c_f} \times \vec{R}_{c_y} \\ \vec{R}_{c_y} \end{pmatrix};$$

$$\$_{d_x} = \begin{pmatrix} \vec{So}_{d_f} \times \vec{R}_{d_x} \\ \vec{R}_{d_x} \end{pmatrix}; \quad \$_{d_y} = \begin{pmatrix} \vec{So}_{d_f} \times \vec{R}_{d_y} \\ \vec{R}_{d_y} \end{pmatrix}; \quad \$_F = \begin{pmatrix} \vec{So}_F \times \vec{F} \\ \vec{F} \end{pmatrix};$$

$$\$_\tau = \begin{pmatrix} \vec{\tau} \\ 0 \end{pmatrix};$$

(8)

To apply the Davies' cutset law [8] the unit network action matrix $[\hat{A}_N]_{\lambda \cdot k \times c}$ is built. In this matrix, the normalized wrenches belonging to each cut *u*, *v* and *w* of the graph GA (Figure 5 (b)) are placed in an organized way. The unit network action matrix for the proposed model is presented in Eq. (9):

$$\$_{a_x} = \begin{matrix} cut\ u \\ cut\ v \\ cut\ w \end{matrix} \begin{bmatrix} \hat{\$}_{a_x} & \hat{\$}_{a_y} & \vec{0} & \vec{0} & \vec{0} & \vec{0} & \hat{\$}_{d_x} & \hat{\$}_{d_y} & \hat{\$}_\tau & \hat{\$}_F \\ \hat{\$}_{a_x} & \hat{\$}_{a_y} & \hat{\$}_{b_x} & \hat{\$}_{b_y} & \vec{0} & \vec{0} & \vec{0} & \vec{0} & \vec{0} & \vec{0} \\ \hat{\$}_{a_x} & \hat{\$}_{a_y} & \vec{0} & \vec{0} & \hat{\$}_{c_x} & \hat{\$}_{c_y} & \vec{0} & \vec{0} & \hat{\$}_\tau & \hat{\$}_F \end{bmatrix} = [\hat{A}_N]_{\lambda \cdot k \times c}$$

(9)

The Davies' *cutset law* states that the sum of the wrenches belonging to a cut is zero [8]. Thus, applied the *cut set law* to the proposed model is obtained the Eq. (10) [8, 11, 12, 24]:

$$\begin{bmatrix} \hat{\$}_{a_x} & \hat{\$}_{a_y} & \vec{0} & \vec{0} & \vec{0} & \vec{0} & \hat{\$}_{d_x} & \hat{\$}_{d_y} & \hat{\$}_\tau & \hat{\$}_F \\ \hat{\$}_{a_x} & \hat{\$}_{a_y} & \hat{\$}_{b_x} & \hat{\$}_{b_y} & \vec{0} & \vec{0} & \vec{0} & \vec{0} & \vec{0} & \vec{0} \\ \hat{\$}_{a_x} & \hat{\$}_{a_y} & \vec{0} & \vec{0} & \hat{\$}_{c_x} & \hat{\$}_{c_y} & \vec{0} & \vec{0} & \hat{\$}_\tau & \hat{\$}_F \end{bmatrix}_{9\times10} \begin{bmatrix} R_{a_x} \\ R_{a_y} \\ R_{b_x} \\ R_{b_y} \\ R_{c_x} \\ R_{c_y} \\ R_{d_x} \\ R_{d_y} \\ \tau \\ F \end{bmatrix}_{10\times1} = [\vec{0}]_{9\times10}$$

(10)

where the first member of the left side of Eq. (10) corresponds to $[\hat{A}_N]_{\lambda \cdot k \times c}$ and the second member of this equation is the matrix of unknowns reactions and torque magnitudes. The system of Eq. (10) can be rewritten [11, 12] so that the *primary network submatrix* $[\hat{A}_{NP}]$ is equal to the last column of the matrix $[\hat{A}_N]_{\lambda \cdot k \times c}$ and the *secondary network submatrix* $[\hat{A}_{NS}]$ is equal to the first nine columns of the matrix $[\hat{A}_N]_{\lambda \cdot k \times c}$. Since $[\hat{A}_{NS}]$ is invertible, the matrix of the unknown reactions and torque magnitudes can be isolated and calculated in Eq. (11):

$$\begin{bmatrix} R_{a_x} \\ R_{a_y} \\ R_{b_x} \\ R_{b_y} \\ R_{c_x} \\ R_{c_y} \\ R_{d_x} \\ R_{d_y} \\ \tau \end{bmatrix}_{9\times1} = -\begin{bmatrix} \hat{\$}_{a_x} & \hat{\$}_{a_y} & \vec{0} & \vec{0} & \vec{0} & \vec{0} & \hat{\$}_{d_x} & \hat{\$}_{d_y} & \hat{\$}_\tau \\ \hat{\$}_{a_x} & \hat{\$}_{a_y} & \hat{\$}_{b_x} & \hat{\$}_{b_y} & \vec{0} & \vec{0} & \vec{0} & \vec{0} & \vec{0} \\ \hat{\$}_{a_x} & \hat{\$}_{a_y} & \vec{0} & \vec{0} & \hat{\$}_{c_x} & \hat{\$}_{c_y} & \vec{0} & \vec{0} & \hat{\$}_\tau \end{bmatrix}^{-1}_{9\times10} \begin{bmatrix} \hat{\$}_F \\ \vec{0} \\ \hat{\$}_F \end{bmatrix}_{9\times10} \cdot \vec{F}$$

(11)

By assigning a value to the primary variable $\vec{F}$, it is possible to obtain a static solution, corresponding to Eq. (11). In order to perform the static simulation that represents the experimental procedure proposed in [7], the motion of the knee flexion ranges from $0^0$ to $90^0$. For each flexion angle, an anterior tibial force $\vec{F}$ is applied. The in-situ force of the ACL is calculated as the force that passes through the link cd for each flexion angle, that is: $F_{ACL\ in-situ} = R_{d_x} / \cos\alpha$. The in-situ force of PCL is calculated as the force that passes through the link ab for each flexion angle, that is: $F_{PCL\ in-situ} = R_{a_x} / \cos\beta$.

## 2.4. Consideration of hyperelastic behavior

This step leads to the identification of forces and length variations of the cruciate ligaments considering hyperelastic behavior. In this step the cruciate ligaments are no longer considered as rigid links, but as a one-dimensional hyperelastic material with length variation as a function of the applied force. The length variation of the links due the hyperelastic behavior, is named in this work, as deformation $\delta$. This deformation $\delta$ has units of length and can be obtained considering the experimental stress-strain curves for one ACL specimen (Figure 6) and its geometric data, as found in [13]. The initial state $\delta = 0$ is defined as the configuration used in the section 2.1.

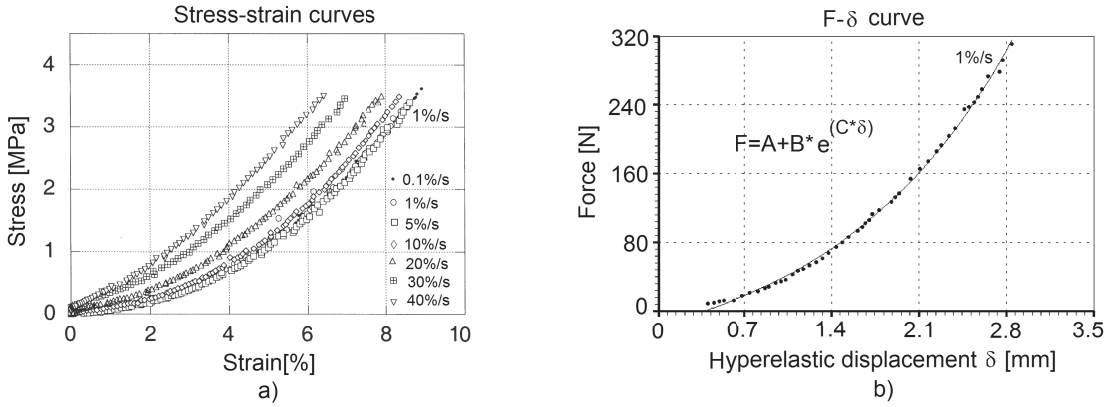


**Figure 6 Experimental data for an ACL specimen: a) Stress-strain data at seven strain rates: , 0.1%/s; ◯, 1%/s; □, 5%/s; ◊, 10%/s; Δ, 20%/s; ⊞, 30%/s; ▽, 40%/s; based on [13]. b) data obtained from a stress-strain rate of 1%/s. This data can be fitted by a hyperelastic constitutive relationship**

Figure 6 (a) shows seven stress-strain curves at different strain rates. The 1%/s strain rate curve was chosen because it is the same strain rate applied in the experimental procedure proposed in [7].

In order to obtain the force-deformation curve $(F_L - \delta)$ from the stress-strain curve, the values of the forces are calculated from the multiplication of the stress values and the magnitude of the cross-sectional area of the ligament $A_0$. In turn, the values of $\delta$ are calculated through the multiplication of the strain values by the length of the unloaded ligament $l_0$. Values of $A_0$ and $l_0$ were obtained from [13]. The curve $F_L - \delta$ obtained for a stress-strain rate of 1%/s is shown in Figure 6 (b).

To determine the mathematical expression that best fi ts the curve $F_L - \delta$ (Figure 6 (b)), a constitutive relationship based on an exponential form can be considered, as shown in Eq. (12):

$$F_L = A + B \cdot e^{\varsigma \cdot \delta} \tag{12}$$

where $F_L$ is the force that passes through the cruciate ligament, $\delta$ is the deformation of the cruciate ligament, $e$ is the Euler number, A, B and $\varsigma$ are constants with values of -0.71, 0.55 and 0.68, respectively. Having A<0 means that there is a compressive force at $\delta = 0$ which is not a problem in this case because magnitude of A is smaller than the smaller value of $F_L$ used in this work and it has, as a consequence, a better fitting of the experimental data. The Eq. (12) can be rearranged in order to provide the term $\delta$ in an explicit way. Therefore, the deformations of the ACL ( $\delta_{ACL}$ ) and PCL ($\delta_{PCL}$) are shown in Eqs. (13) and (14) respectively, where $F_{ACL}$ is the force that passes through the ACL and $F_{PCL}$ is the force that passes through the PCL.

$$\delta_{ACL} = \ln\left(\left(F_{ACL} - A\right)/B\right)\varsigma^{-1} \tag{13}$$

$$\delta_{PCL} = \ln\left(\left(F_{PCL} - A\right)/B\right)\varsigma^{-1} \tag{14}$$

The in-situ forces in the cruciate ligaments ($F_{ACL\ in-situ}$ and $F_{PCL\ in-situ}$) are solved in the previous step of the proposed methodology, considering the ligaments as rigid links. These values of forces are then used to substitute $F_{ACL}$ and $F_{PCL}$ in Eqs. (13) and (14), respectively, in order to obtain the values for the corresponding deformations $\delta_{ACL}$ and $\delta_{PCL}$, for each flexion angle.

It is important to note that each deformation ($\delta_{ACL}$ and $\delta_{PCL}$) varies with the in-situ force for each flexion angle. All of the successive ligament positions (considering rigid links) have to be updated, as shown in Eqs. (15) and (16) considering these deformations:

$$\vec{So}_{c_f\,(hyperelastic)} = \vec{So}_{c_f} + \delta_{ACL} \tag{15}$$

$$\vec{So}_{b_f\,(hyperelastic)} = \vec{So}_{b_f} + \delta_{PCL} \tag{16}$$

where the updated positions of the ACL and PCL, now considering hyperelastic behavior, are called $\vec{S}o_{c_f\,(hyperelastic)}$ and $\vec{S}o_{b_f\,(hyperelastic)}$ respectively. Three principal successive positions of the cruciate ligaments, considering hyperelastic behavior (thin line) and considering the ligaments a rigid links (thick line), are shown in (Figure 7).

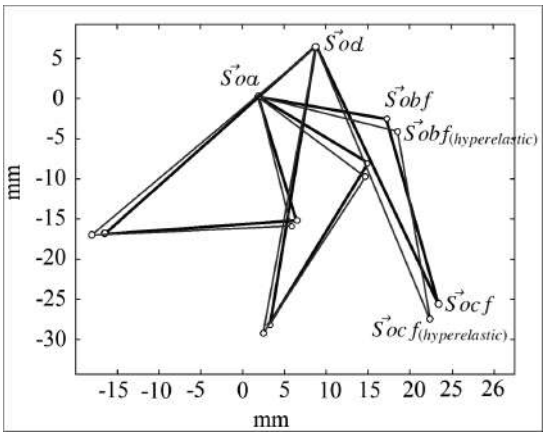


**Figure 7** Positions of the cruciate ligaments: considering hyperelastic behavior (thin line) and considering the ligaments as rigid links (thick line)

For the updated positions the *cutset law* is reapplied to finding the in-situ forces that consider hyperelastic behavior of the cruciate ligaments, as will be shown in the next section.

# 3. Results

In this section, the experimental and simulated results for the in-situ forces in the ACL are presented. In Figure 8 are shown the results for an anterior tibial load of $F_1$ = 110N.

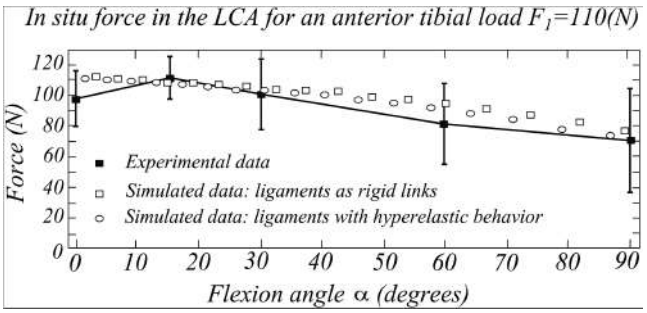


**Figure 8** In-situ forces in the ACL for an anterior tibial load F1=110N: ■ experimental values from [7] with its standard deviation; ○ values simulated considering the ligaments as rigid links (neglecting hyperelastic behavior); and □ values simulated considering hyperelastic

In this figure, the experimental values were obtained in [7] where an anterior tibial load $F_1$ is robotically applied to the following flexion angles: $0^0$, $15^0$, $30^0$, $60^0$, $90^0$. The simulated results are obtained considering that $F_1$ is continuously applied from $0^0$ up to $90^0$. In Figure 8 the experimental values are shown in black squares, the simulated values considering hyperelastic behavior are in circles and the simulated values considering the ligaments as rigid links are in white squares. The maximum differences between the experimental and simulated values for the in-situ force occur at flexion of $60^0$ and $0^0$.

Following this procedure, the in-situ forces in the ACL were evaluated for the same flexion angles, but varying the magnitude of the anterior tibial loads $F_1$ to: 110N, 88N, 66N, 44N and 22N. The experimental values are shown in Figure 9 (a). The simulated values considering the ligaments as rigid links are shown in Figure 9 (b). The simulated values considering hyperelastic behavior are shown in Figure 9 (c).

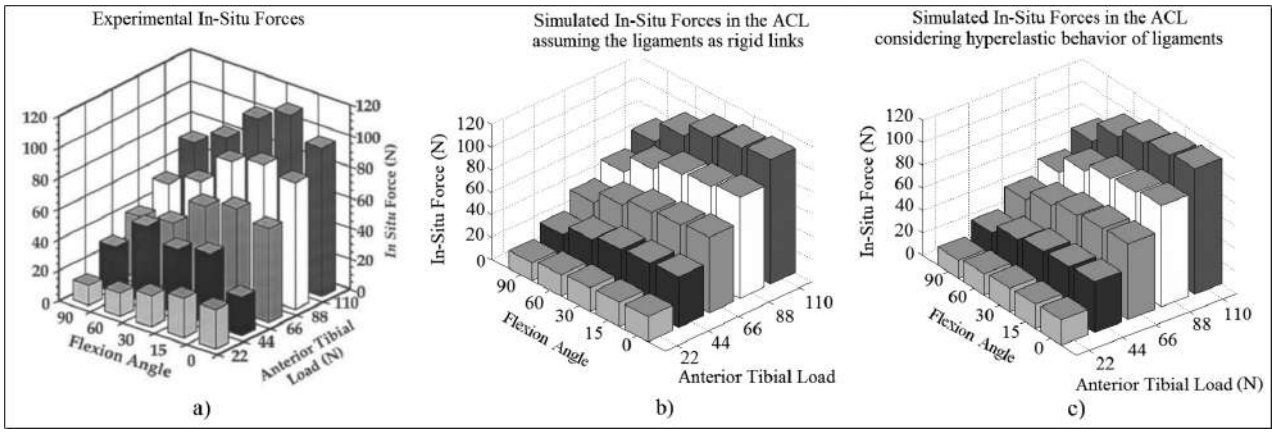


**Figure 9** In-situ forces for F1 magnitudes: a) experimental values [7], b) values simulated considering the ligaments as rigid links (neglecting hyperelastic behavior), and c) values simulated considering hyperelastic behavior

# 4. Discussion

Comparing the simulated values in Figure 8, the ACL in-situ force obtained by modeling the cruciate ligaments as rigid links shows similar results to the ones obtained by considering hyperelastic behavior. It can be explained by the small values of deformation. It leads to small variations of the geometric configuration between the rigid link model and the hyperelastic model (Figure 7). These small variations result in a close proximity between the forces of each model (Eq. 11).

Comparing the experimental ACL in-situ force and the simulated values obtained in a two-dimensional four bar model (Figure 8) a similar tendency is observed, except in the full extension region (0° of flexion). The proposed model with its assumptions numbered in section 2.1 produces simulated values of in-situ force within the standard deviation of the experimental values.

The following definitions for error (Eqs. 17 and 18) were used to analyze the bar graphs in Figure 9.

$$e_{ex}=\sum_{i}^{n}\frac{\left|Esperimental\ data_i-Simulated\ data_i\right|}{Esperimental\ data_i\cdot n}\cdot 100 \tag{17}$$

$$e_{sim}=\sum_{i}^{n}\frac{\left|Esperimental\ data\ (\text{rigid})_i-Simulated\ data\ (\text{hyperelastic})_i\right|}{Esperimental\ data\ (\text{rigid})_i\cdot n}\cdot 100 \tag{18}$$

In these equations i = 1,...,n where n is the number of flexion angles evaluated. The error $e_{ex}$ (Eq. 17) is calculated between experimental and simulated values. The error $e_{sim}$ is calculated between simulated values (Eq. 18). The errors $e_{ex}$ and $e_{sim}$ are shown in Table 1.

**Table 1** Errors between data of Figure 9 for the whole set of anterior tibial loads, where Exp: experimental data; Rigid: simulated data for rigid links; Hyp: simulated data for hyperelastic links

| | Data | $F_1$=22N | $F_1$=44N | $F_1$=66N | $F_1$=88N | $F_1$=110N | Total mean |
|---|---|---|---|---|---|---|---|
| $e_{ex}$ % | Exp-Rigid | 16.18 | 21.47 | 9.34 | 7.87 | 6.39 | 12.25 |
| $e_{ex}$ % | Exp-Hyp | 16.33 | 20.60 | 11.53 | 9.41 | 8.65 | 13.30 |
| $e_{sim}$ % | Rigid-Hyp | 0.45 | 1.12 | 2.74 | 1.79 | 2.63 | 1.74 |

In Table 1, it can be observed how close the experimental values are to the simulated values, for the whole set of anterior tibial loads. Here, it is observed that $e_{ex}$ for rigid links is smaller than $e_{ex}$ for hyperelastic links. Considering this fact and that $e_{sim}$ is very small, the hyperelastic behavior would be neglected. It can also be seen that while $F_1$ increases, $e_{ex}$ decreases and $e_{sim}$ has a tendency to grow, it can be explained because the deformation is also increased. Finally, is expected that $e_{sim}$ decreases while the strain rate grows (Figure 6), for the same $F_1$.

# 5. Conclusions

In the proposed simulation of the ACL in-situ force, the modeling of the cruciate ligaments as rigid links shows similar results to the modeling which considers the hyperelastic behavior, in agreement with the first hypotheses, presenting a total mean of the errors $e_{sim}$ very small (1.74%). Considering the above claimed and that the total mean value of $e_{ex}$ for rigid links data is lower than the $e_{ex}$ for hyperelastic data, it can be stated that the inclusion of the hyperelastic behavior can be neglected.

The proposed model of the human knee joint, modeled as a two-dimensional four bar mechanism, provides results for the position and in-situ forces in the ACL which are close to the corresponding experimental data, in concordance to the second hypotheses proposed. Therefore, it can be concluded that: If two rigid links representing the ligaments were in fact replaced by ligaments, the difference between the two models would be very small. Thus, the proposed model could provide support to orthopedic surgeons with information, which is important for the preoperative planning and medical decision making.

The proposed methodology for the inclusion of hyperelastic behavior could be considered as a series of iterations, where the positions of the ligaments are accommodated until they converge, according to an external load $F_1$ and the deformation $\delta$ in the constitutive relationship (Eq. 12). However, in this work a single iteration was performed, because the variation in the length of the ligaments in just one iteration was very small, and thus it was considered that convergence had been reached.

One possible reason of the difference between the simulated and experimental results for the in-situ forces in the ACL is the neglecting of the three-dimensional effects, such as the axial rotation of the knee.

Despite the simplicity of the model, it has provided a good agreement with the experimental results. The proposed methodology would allow the present model to be improved in future works, simulating customized models of the knee, including three dimensional effects and other internal structures, which will allow better results to be obtained with values closer to the experimental data.6.

# 6. Acknowledgements

The authors would like to thank the CAPES - Coordenação de Aperfeiçoamento de Pessoal de Nível Superior and CNPq - Conselho Nacional de Desenvolvimento Científico e Tecnológico, Brazil, that provided financial support for this research.

# 7. References

1. S. Woo, C. Wu, O. Dede, F. Vercillo, S. Noorani. "Biomechanics and anterior cruciate ligament reconstruction". *Journal of Orthopaedic Surgery and Research*. Vol. 1. 2006. pp. 1-9.
2. K. Olanlokun, D. Wills. "A spatial model of the knee for the preoperative planning of knee surgery". Proceedings of the Institution of Mechanical Engineers, Part H: Journal of Engineering in Medicine. Vol. 216. 2002. pp. 63-75.
3. N. Sancisi, V. Parenti. "A 1 dof parallel spherical wrist for the modelling of the knee passive motion". *Mechanism and Machine Theory*. Vol. 45. 2010. pp. 658-665.
4. A. Ottoboni, V. Parenti, A. Leardini. *On the limits of the articular surface approximation of the human knee passive motion models*. Proceedings of the 17th AIMeTA Congress of Theoretical and Applied Mechanics. Firenze, Italy. 2005. pp. 1-11.
5. N. Sancisi, D. Zannoli, V. Parenti, C. Belvedere, A. Leardini. "A one-degree-of-freedom spherical mechanism for human knee joint modelling". *Proceedings of the Institution of Mechanical Engineers, Part H: Journal of Engineering in Medicine*. Vol. 225. 2011. pp. 725-735.
6. S. Woo, S. Abramowitch, R. Kilger, R. Liang. "Biomechanics of knee ligaments: injury, healing, and repair". *Journal of biomechanics.* Vol. 39. 2006. pp. 1-20.
7. S. Woo, R. Fox, M. Sakane, G. Livesay, T. Rudy, F. Fu. "Biomechanics of the ACL: Measurements of in-situ force in the ACL and knee kinematics". *The Knee*. Vol. 5. 1998. pp. 267-288.
8. T. Davies. "Freedom and constraint in coupling networks". *Proceedings of the Institution of Mechanical Engineers, Part C: Journal of Mechanical Engineering Science*. Vol. 220. 2006. pp. 989-1010.
9. T. Davies. "Circuit actions attributable to active couplings". *Mechanism and Machine Theory*. Vol. 30. 1995. pp. 1001-1012.
10. L. Laus, H. Simas, D. Cruz, D. Martins. "Efficiency of gear trains determined using graph and screw theories". *Mechanism and Machine Theory*. Vol. 1. 2012. pp. 296-325.
11. D. Ponce, C. Roesler, D. Martins. "A human knee joint model based on screw theory and its relevance for preoperative planning". *Mecánica Computacional*. Vol. 31. 2013. pp. 3847-3871.
12. D. Ponce, D. Martins, C. Roesler, F. Rosa, A. Ocampo. *Modeling of human knee joint in sagittal plane considering elastic behavior of cruciate ligaments*. Proceedings of the 22nd International Congress of Mechanical Engineering (COBEM). São Paulo, Brazil. 2013. pp. 5853-5864.
13. D. Pioletti, L. Rakotomanana, P. Leyvraz. "Strain rate effect on the mechanical behavior of the anterior cruciate ligament–bone complex". *Medical Engineering & Physics*. Vol. 21. 1999. pp. 95-100.
14. J. O'Connor, T. Shercliff, E. Biden, J. Goodfellow. "The geometry of the knee in the sagittal plane". *Proceedings of the Institution of Mechanical Engineers, Part H: Journal of Engineering in Medicine*. Vol. 203. 1989. pp. 223-233.
15. J. O'Connor, A. Zavatsky. "ACL function in the normal knee". *Biomecánica*. Vol. 3. 1995. pp. 121-132.
16. P. Williams, G. Peura, A. Hoffman. *A model of knee motion in the sagittal plane*. Proceedings of the IEEE Seventeenth Annual Northeast, Bioengineering Conference. Worcester, USA. 1991. pp. 273-274.
17. J. Bradley, D. Fitzpatrick, D. Daniel, T. Shercliff, J. O'Connor. "Orientation of the cruciate ligament in the sagittal plane". *Journal of Bone and Joint Surgery*. Vol. 70. 1988. pp. 94-99.
18. B. Clement, G. Drouin, G. Shorrock, P. Gely. "Statistical analysis of knee ligament lengths". Journal of Biomechanics. Vol. 22. 1989. pp. 767-774.
19. R. Crowninshield, M. Pope, R. Johnson. "An analytical model of the knee". *Journal of Biomechanics*. Vol. 9. 1976. pp. 397-405.
20. C. Wang, P. Walker, B. Wolf. "The effects of flexion and rotation on the length patterns of the ligaments of the knee". Journal of Biomechanics. Vol. 6. 1973. pp. 587-592.
21. F. Freudenstein. "Approximate synthesis of four-bar linkages". *Resonance*. Vol. 15. 2010. pp. 740-767.
22. J. Selig. "Rigid Transformations". *Introductory Robotics*. 1st ed. Ed. Prentice Hall. London, UK. 1992. pp. 7-18.
23. L. Tsai. "Basic Concepts of Graph Theory". *Mechanism Design: Enumeration of Kinematic Structures According to Function*. 1st ed. Ed. CRC Press LLC. New York, USA. 2001. pp. 33-58.
24. T. Davies. "Mechanical networks—iii wrenches on circuit screws". *Mechanism and Machine Theory.* Vol. 18. 1983. pp. 107-112.